

Variable-Depth Liner Evaluation Using Two NASA Flow Ducts

M. G. Jones*, D. M. Nark†, W. R. Watson‡ and B. M. Howerton§

NASA Langley Research Center, Hampton, VA 23681

Four liners are investigated experimentally via tests in the NASA Langley Grazing Flow Impedance Tube. These include an axially-segmented liner and three liners that use re-ordering of the chambers. Chamber reordering is shown to have a strong effect on the axial sound pressure level profiles, but a limited effect on the overall attenuation. It is also shown that bent chambers can be used to reduce the liner depth with minimal effects on the attenuation. A numerical study is also conducted to explore the effects of a planar and three higher-order mode sources based on the NASA Langley Curved Duct Test Rig geometry. A four-segment liner is designed using the NASA Langley CDL code with a Python-based optimizer. Five additional liner designs, four with rearrangements of the first liner segments and one with a redistribution of the individual chambers, are evaluated for each of the four sources. The liner configuration affects the sound pressure level profile much more than the attenuation spectra for the planar and first two higher-order mode sources, but has a much larger effect on the SPL profiles and attenuation spectra for the last higher-order mode source. Overall, axially variable-depth liners offer the potential to provide improved fan noise reduction, regardless of whether the axially variable depths are achieved via a distributed array of chambers (depths vary from chamber to chamber) or a group of zones (groups of chambers for which the depth is constant).

I. Introduction

As the volume of air traffic continues to increase, there is constant pressure to reduce aircraft noise in the vicinity of airports. In response to this pressure, the International Civil Aviation Organization and Federal Aviation Administration continue to impose increasingly stringent noise requirements regarding the noise produced by aircraft during takeoff and landing operations. For approximately six decades, acoustic liners have been employed for the reduction of fan noise, which is a significant contributor to aircraft noise. These liners have generally consisted of single-degree-of-freedom (SDOF) or double-degree-of-freedom (DDOF) configurations tuned to absorb selected tones (e.g., multiples of the blade passage frequency).

Aircraft engine bypass ratios have increased significantly over the last few decades. Whereas the fan noise was tone dominated for the lower bypass ratio engines, it now consists of a combination of tones and broadband noise. The amount of space suitable for acoustic liner installation has also decreased. Thus, there is increased interest in acoustic liner concepts that offer the potential for increased broadband noise reduction. One such liner concept is the axially-segmented (zone) liner, which employs a small number of uniform-impedance segments over the axial extent of the liner. This type of liner has been considered by many researchers.^{1–8} Each axial segment is designed such that the total effect is improved broadband absorption. For example, one axial segment may be used to transfer energy from one mode to another, such that a subsequent axial segment can provide more effective sound absorption.

In 2014, the NASA Langley Research Center Liner Physics Team began investigation of a slight variation of this concept. Instead of employing a small number of axial segments, each of which consists of a uniform

*Senior Research Scientist, Research Directorate, Structural Acoustics Branch, AIAA Associate Fellow.

†Senior Research Scientist, Research Directorate, Structural Acoustics Branch, AIAA Associate Fellow.

‡Senior Research Scientist, Research Directorate, Computational AeroSciences Branch, AIAA Associate Fellow.

§Research Scientist, Research Directorate, Structural Acoustics Branch, AIAA Senior Member.

impedance configuration, this concept allows the impedance to be varied with a much finer axial resolution. This impedance variability is achieved by varying the depth of the individual chambers of the full liner. The first study⁷ consisted of tests conducted in the NASA Langley Grazing Flow Impedance Tube (GFIT) to evaluate a variable-depth ceramic matrix composite acoustic liner. Two propagation codes were validated via comparisons of predicted and measured acoustic pressure profiles for this variable-depth liner.

For the second study,⁸ two variable-depth liners were experimentally evaluated using the GFIT. The first liner consisted of chambers with depths that varied linearly from the leading edge to the trailing edge. The second contained linearly, axially varying chamber depths over the first half of the liner, and the chamber depths were constant over the remainder of the liner. Favorable comparisons of predicted and measured axial acoustic pressure (sound pressure level (SPL) and phase) profiles were used to validate the impedance prediction model and acoustic propagation codes, with and without the effects of grazing flow included. Also, the orientation of these liners (liner orientation could be reversed) was demonstrated to affect the details of the axial acoustic pressure profile, but to have minimal effect on the total amount of attenuation in the GFIT. The impedance prediction model and propagation codes were also used to explore the predicted effects of a number of distinct liner configurations.

In 2016, three acoustic propagation codes were used to further explore variable-depth liner configurations.⁹ A numerical study was used to demonstrate that it is acceptable to treat a variable impedance as uniform (smeared) if the spatial extent over which this variable impedance occurs is less than one-third of a wavelength of the incident sound. An optimization study was used to design a liner with much finer chamber depth resolution for the Mach 0.0 and 0.3 test conditions. Two liners were designed and fabricated based on spatial rearrangement of chambers from this liner, and were tested in the GFIT for the Mach 0.0 condition. Predicted and measured attenuations were shown to compare favorably across the full frequency range. However, these liners could not be tested with flow due to facility constraints. During this past year, modifications have been implemented such that these liners can now be tested in the GFIT with flow.

The purpose of the current study is to extend the evaluation of the two variable-depth liners⁹ to include the effects of Mach 0.3 grazing flow. Two additional variable-depth liners are explored, with and without grazing flow. These new liners employ bent chambers to allow the full liner thickness to be decreased significantly, while maintaining the same individual chamber depths of the earlier liner, albeit with a different axial distribution of chamber depths. Finally, it should be noted that the acoustic source in the GFIT typically consists solely of a plane wave. Hence, it is important to explore whether variable impedance liner benefits exist for a variety of sound sources. As an initial step toward this goal, an optimized variable-depth zone liner is designed for implementation in the NASA Langley Curved Duct Test Rig (CDTR). A propagation code is then used to compare attenuation spectra predicted for this zone liner, and for a number of reconfigurations of this liner, for a variety of sound sources.

This paper is organized as follows. The two aeroacoustic propagation codes that are used to validate results for this study are briefly described in Section II. Section III provides a description of the two test rigs (GFIT and CDTR) and the liner configurations considered in this study. Results are provided in Section IV, and concluding remarks are provided in Section V.

II. Duct Acoustic Propagation Codes

Two duct acoustic propagation codes (CHE¹⁰ and CDL¹¹) are used in this study. These codes are described in detail in the cited references, so only those details that are key to the current study are provided herein. Each of these codes solves the convected Helmholtz equation and, for the purposes of this study, employs a uniform flow profile. They also allow the liner to be installed on either the upper wall (as in the GFIT) or the side wall (as in the CDTR). Further, the CHE code is extended to quasi-3D, so that it can accommodate the higher-order vertical modes that are cut on in the larger cross-section of the CDTR. Both propagation codes allow the impedance to vary along the axial length of the liner. The modified CHE code solves a partial differential equation on the acoustic pressure, includes the effects of reflections at the leading and trailing edges of the liner, and has the potential to capture reflections at the duct termination. The CDL propagation code utilizes a parabolic approximation to the convected Helmholtz equation with the acoustic potential as the unknown variable. The CDL code is a computationally efficient model that accounts for three-dimensional geometries. However, it neglects reflections due to impedance discontinuities at the leading and trailing edges of the liner. It also assumes the duct termination to be anechoic.

III. Experimental Method

This section provides information regarding features of the GFIT and CDTR that are pertinent to the current study. A description of each test rig, as well as the liners used (whether real or simulated) with each test rig is also included.

A. Grazing Flow Impedance Tube

The GFIT (Fig. 1) has a cross-sectional geometry of 2.0" wide by 2.5" high, and allows evaluation of acoustic liners with lengths from 2.0 to 24.0". The surface of the test liner forms a portion of the upper wall of the flow duct. Twelve acoustic drivers form an upstream (exhaust mode) source section. For this study, these drivers are used to generate tones (one frequency at a time) over a frequency range of 400 to 3000 Hz, at source levels (measured at the reference microphone) of 120 and 140 dB, and at centerline Mach numbers of 0.0 and 0.3. Fifty-three (53) microphones are flush-mounted in the lower wall (opposite the liner) of the GFIT, and are used to measure the acoustic pressure field over the axial extent of $\{0 \leq x \leq L\}$. Here, x is the axial coordinate and L denotes the length of the duct from the source to the exit plane.

For this study, the source plane (plane in which the reference microphone is located) is at $x = 0$ ", the leading edge of the liner is at $x = 8$ ", and the termination plane (plane in which the farthest downstream microphone is located) is at $x = 40$ ".

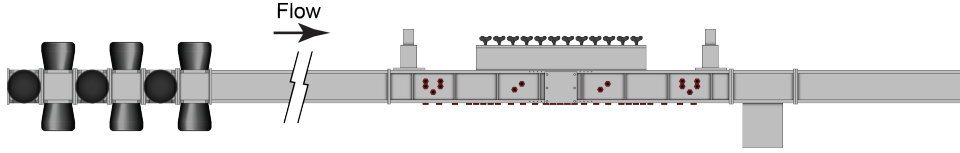


Figure 1: Sketch of Grazing Flow Impedance Tube (GFIT).

B. Grazing Flow Impedance Tube Liner Configurations

Four 2.0"-wide by 17.1"-long liner configurations, labeled as C1, C2, C3, and C4, are evaluated in this study (see Figs. 2 and 3). Each liner consists of a 3×24 array of square (0.6" \times 0.6") chambers separated by 0.1"-wide axial and spanwise partitions. A 270 MKS Rayls (0.65 ρc -units) wire mesh facesheet^a is used with each liner. Thus, the surface impedance,^b ζ_i , of the i^{th} chamber is given by

$$\zeta_i = 0.65 - j \cot(kd_i), \quad (i = 1, 24) \quad (1)$$

where j is the unit imaginary number, k represents the freespace wavenumber, and d_i denotes the depth of the i^{th} chamber in the axial direction (each chamber in the spanwise dimension has the same depth). The freespace wavenumber is given by

$$k = \omega/c \quad (2)$$

where $\omega = 2\pi f$ is the angular frequency and f is the excitation frequency in Hertz. Figure 3 provides top and side view sketches of the four liners.

As mentioned earlier, the C1 and C2 liners were designed as part of an earlier study.⁹ The CDL code was used with an optimizer developed using the Python programming language^{12,13} to design the C1 liner. For this design optimization, the axial length of the liner was assumed to be divided into eight equal-length axial segments, and each segment consisted of an array of 3×3 identical chambers. The design was optimized

^aFacesheet normalized resistance was erroneously reported as 0.5 in earlier report.⁹

^bAn $e^{i\omega t}$ time convention is assumed. Also, all impedances in this paper are assumed normalized by ρc , where ρ and c represent the density and sound speed of air, respectively.

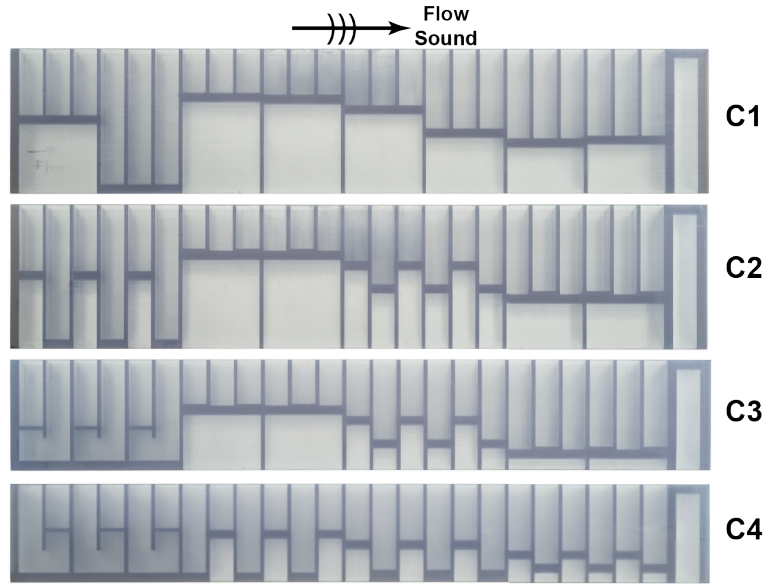


Figure 2: Photograph of four GFIT liners (C1 - C4). The wire mesh facesheet at the top surface of each liner is not shown. C1 - optimized zone liner with variable-depth chambers; C2 - chambers of C1 reordered; C3 - implement folded-cavities to reduce liner depth; C4 - reorder for more efficient packaging. Side view.

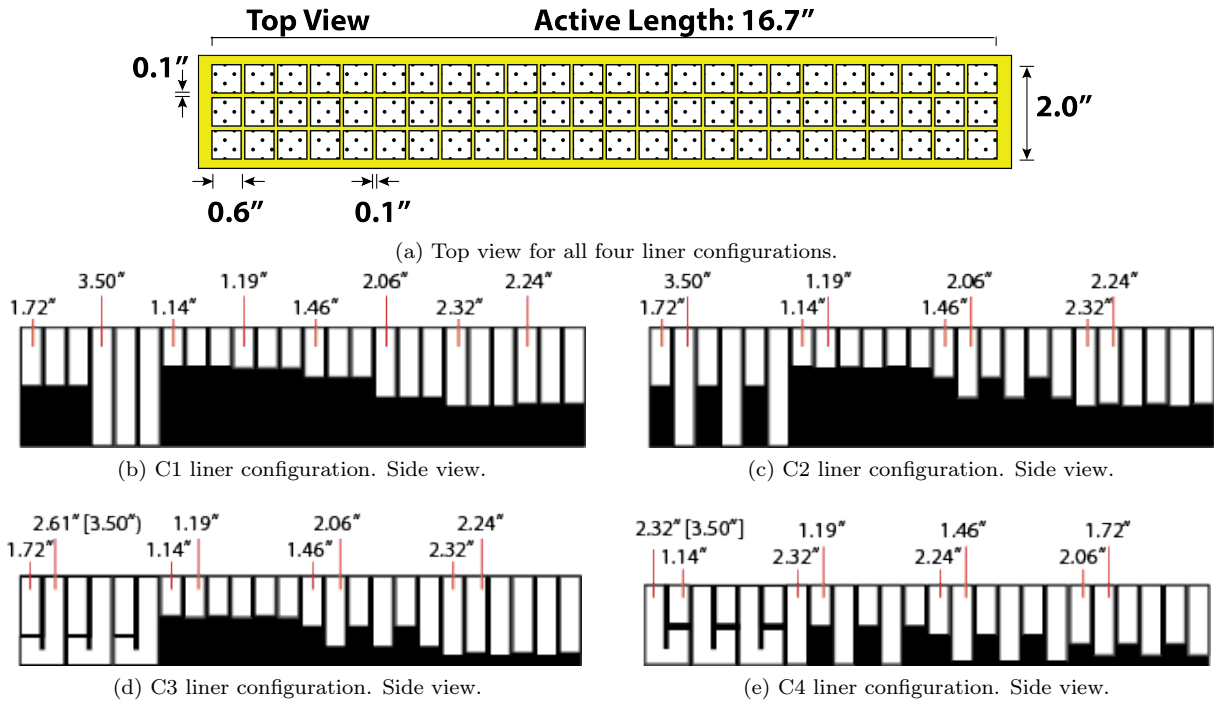


Figure 3: Sketch of liner configurations C1 - C4. Dimensions provided in parts (b) - (e) represent chamber heights. Total lengths of bent chambers are provided in brackets.

to maximize the amount of attenuation at Mach 0.0 and over the frequency range of 1000 to 3000 Hz. The attenuation, A_f , at an individual frequency is simply computed as

$$A_f = \text{SPL}_s - \text{SPL}_t \quad (3)$$

where SPL_s and SPL_t represent the sound pressure levels (dB) at the source ($x = 0''$) and termination ($x = 40''$) planes, respectively. Chamber depths were allowed to vary over the range of 1.0'' to 4.0''. The higher fidelity CHE code was then used to confirm the selected configuration. For the C2 liner, the chambers from each successive pair of segments in the C1 liner were interleaved (maintained constant depth for spanwise set of chambers).

Each of these liners was built by the NASA Langley Additive Manufacturing Center using a stereolithography process and tested in the GFIT for the Mach 0.0 condition. The measured data were shown to compare favorably with the acoustic pressures predicted with the two propagation codes. This confirmed that each of the propagation codes could be acceptably used to design axially variable-depth liners, at least for the no-flow condition with a plane-wave source. It also demonstrated that the ordering of the chambers affected the axial profile of sound pressure level, but had minimal effect on the total amount of attenuation for samples mounted in the GFIT. In the current study, the C1 and C2 liners are tested in the GFIT at Mach 0.3.

The C3 liner is nearly identical to the C2 liner. The only difference is the use of bent chambers to replace the longest chambers (3.50'' total length). As shown in Figure 3, the total depth of this sample is 2.61'', the depth of the first portion of the bent chamber. The purpose of this liner is to determine whether bent chambers can be properly modeled as straight chambers with a length corresponding to the total length of the unwrapped chamber. Clearly, the use of bent chambers reduces the overall liner depth, which offers benefits regarding reduced weight and, thereby, fuel requirements.

The C4 liner further employs the use of reordering to minimize the total depth of the liner. By pairing the longest and shortest chambers in successive pairs of chambers over the length of the liner, the total depth is reduced to 2.32''. When compared to the C2 liner, which does not employ bent chambers, this represents *a 34% decrease in the total depth of the liner.*

C. Curved Duct Test Rig

The CDTR (see Figure 4) has a cross-sectional geometry of 6.0'' wide by 15.0'' high, and allows evaluation of acoustic liners with lengths up to 32.0''. These liners can be mounted on the left, right, or both side walls of the duct, and the surface of these liners forms the side wall(s) of the duct. Thirty-two (32) acoustic drivers (not shown in Fig. 4) form an upstream source section. As with the GFIT, these drivers are used to generate tones over a frequency range of 400 to 3000 Hz, at source levels of approximately 130 dB, and at centerline Mach numbers of 0.0 to 0.5. One hundred fifty-eight (158) microphones are flush-mounted in the CDTR walls. Sixty-three (63) are mounted in the upstream array, sixty-three (63) are mounted in the downstream array, and thirty-two (32) are mounted in the lid array. The upstream and downstream microphone arrays are used to determine the modal content of the acoustic field in the upstream and downstream hard-wall sections.

One key feature of the CDTR is the ability to control the mode content at the upstream end of the duct. This is achieved by independent control of the amplitude and phase of the electronic signals feeding each of the acoustic drivers. A control system is employed to use a portion of the upstream array of microphones to provide feedback to guide the proper selection of these amplitudes and phases, such that the target mode is at least 10 dB above all other modes in the upstream hard wall section.

D. Curved Duct Test Rig Liner Configuration

In a manner similar to that used earlier for the GFIT liner optimization, the CDL code was used with an optimizer developed using the Python programming language^{12,13} to design a 14.0''-wide by 30.0''-long (active area) axially-segmented (zone) liner for the CDTR. Although the eventual goal is to build this liner for experimental evaluation, the current results are limited to a numerical study. The goal for this design process was to maximize the attenuation achieved with the (0,0)-mode (plane wave) for the no-flow (Mach 0.0) condition. This liner consists of a 28×60 array of square (0.4'' \times 0.4'') chambers separated by



Figure 4: Photograph of Curved Duct Test Rig (CDTR) test section.

0.1"-wide axial and spanwise partitions. Axially, the liner is divided into four equal-length (7.5") segments. It has a conventional perforate facesheet, with a hole diameter of 0.040" and a sheet thickness of 0.032". Each segment of this liner consists of a 28×15 array of chambers with constant chamber depths. Thus, there were five optimization parameters for this design - the open area ratio of the facesheet ($0.04 \leq \sigma \leq 0.16$) and the individual depths ($1" \leq \{d_1, d_2, d_3, d_4\} \leq 4"$) of the chambers that form the four equal-length segments. As a result of this process, the optimized liner design parameters were determined to be $\sigma = 0.10$, $d_1 = 1.00"$, $d_2 = 2.00"$, $d_3 = 3.92"$, and $d_4 = 1.86"$.

In Section IV, the CDL propagation code is used to evaluate the effects of different test conditions (multiple higher-order mode sources, at Mach 0.0 and 0.3) on the acoustic performance of this liner configuration (labeled as Zone1). Five additional liner configurations are also considered (Fig. 5). The geometric parameters for each of these configurations are provided in Table 1.

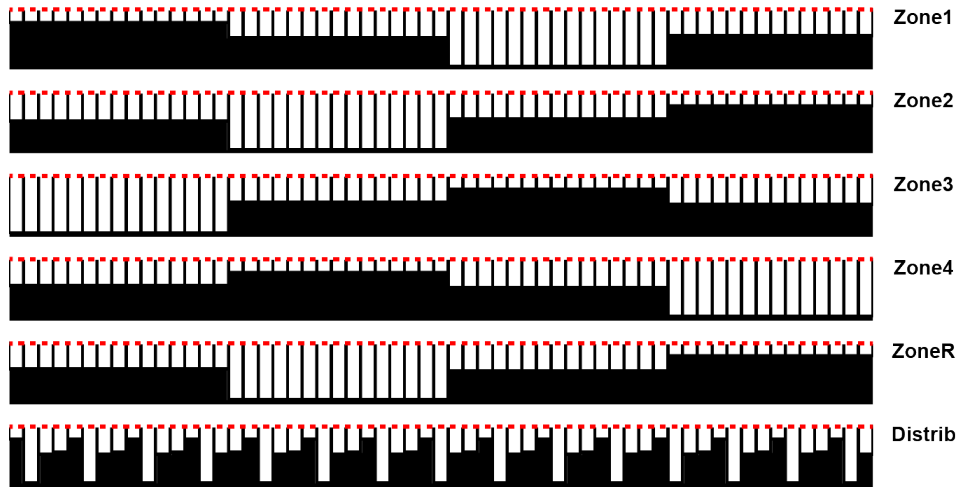


Figure 5: Sketches of six CDTR liner configurations. Side View.

Table 1: Geometric parameters for CDTR liner configurations.

Label	d_1	d_2	d_3	d_4	σ
Zone1	1.00"	2.00"	3.92"	1.86"	0.10
Zone2	2.00"	3.92"	1.86"	1.00"	0.10
Zone3	3.92"	1.86"	1.00"	2.00"	0.10
Zone4	1.86"	1.00"	2.00"	3.92"	0.10
ZoneR	1.86"	3.92"	2.00"	1.00"	0.10
Distrib	1.00"	3.92"	2.00"	1.86"	0.10

Configurations Zone2 - Zone4 consist of the same 7.5"-long segments as are used in the Zone1 configuration, albeit with different ordering (cyclic permutation). The ZoneR configuration is simply the reverse orientation of the Zone1 configuration. The last liner, labeled as Distrib, consists of chambers with the same four depths. For this configuration, the depths of segments 1 and 3 of the Zone1 configuration are employed for the first two axial chambers (for convenience, all chambers in the spanwise dimension are identical for all liners considered in this study). The depths of Zone1 segments 2 and 4 are employed for the next two axial chambers, and this ordering of chamber depths is replicated over the full length of the Distrib configuration. This ordering of chambers was chosen to place the longest and shortest chambers axially adjacent to one another, such that bent chambers could be efficiently employed to reduce the overall depth of the liner.

IV. Results and Discussion

Results acquired in the GFIT with four liners (labeled as C1 - C4) are provided in this section. Results from a numerical study of the six CDTR liner configurations (labeled as Zone1 - Zone4, ZoneR, and Distrib) are also presented.

A. Grazing Flow Impedance Tube Results

Two liners (C1 and C2) were tested at Mach 0.0 in the GFIT as part of an earlier study.⁹ Figure 6 provides a comparison of SPL axial profiles measured with source levels of 120 dB and 140 dB for the C1 liner. Results are shown for frequencies of 1000, 1400, 1800, and 2200 Hz. These frequencies are chosen to cover the frequency range of interest while ensuring that the sound field is limited to plane waves at the source and exit planes of the test window. As should be expected for a linear liner (recall that the facesheet is a wire mesh), the effects of source SPL on the axial profiles are negligible. Therefore, the remainder of the results will be limited to tests conducted with a source SPL of 140 dB.

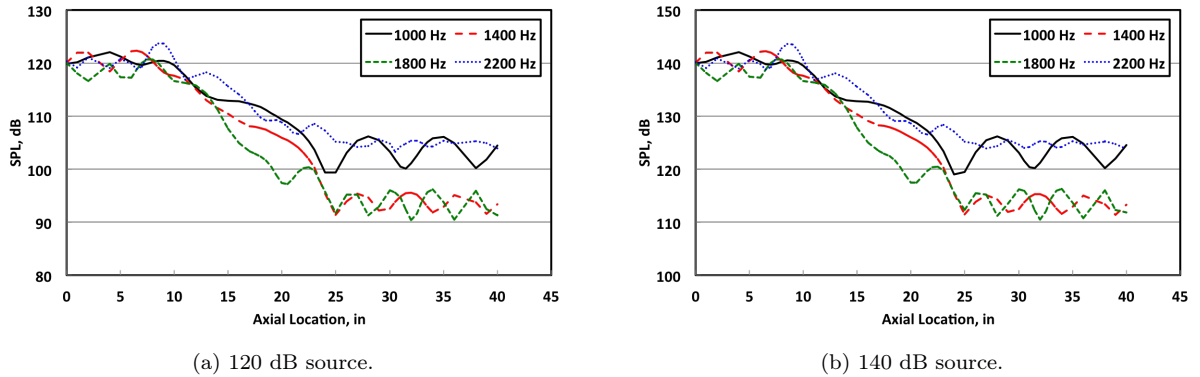


Figure 6: SPL axial profile, C1 liner. Mach 0.0.

Figure 7 provides a comparison of measured attenuation spectra for all four liners, for flow conditions of Mach 0.0 and 0.3, respectively. The legend indicates the liner (C1 - C4), the target Mach number (M0 and M3 denote Mach 0.0 and Mach 0.3, respectively), and the source SPL (L4 denotes 140 dB). The attenuation spectra compare favorably for all four liners, especially for frequencies for which only the plane wave carries energy in the hard wall section downstream of the liner, i.e., up to 2600 Hz at Mach 0.0 and 2400 Hz at Mach 0.3. However, there are definitely some effects of liner configuration on the measured attenuation.

Recall that this metric is very simplistic, computed as the difference between the total SPL at the source and exit planes. Thus, the attenuation reported herein is simply a transmission loss. Since the sound field is generated via a set of acoustic drivers upstream of the liner, standing waves are generated due to reflections from the leading edge of the liner. There are also standing waves generated by reflections at the liner trailing edge and at the physical termination of the duct (at the downstream diffuser leading edge). Given the presence and variability of these reflections, the comparisons (see Fig. 7) of attenuation spectra for the different liners is quite favorable.

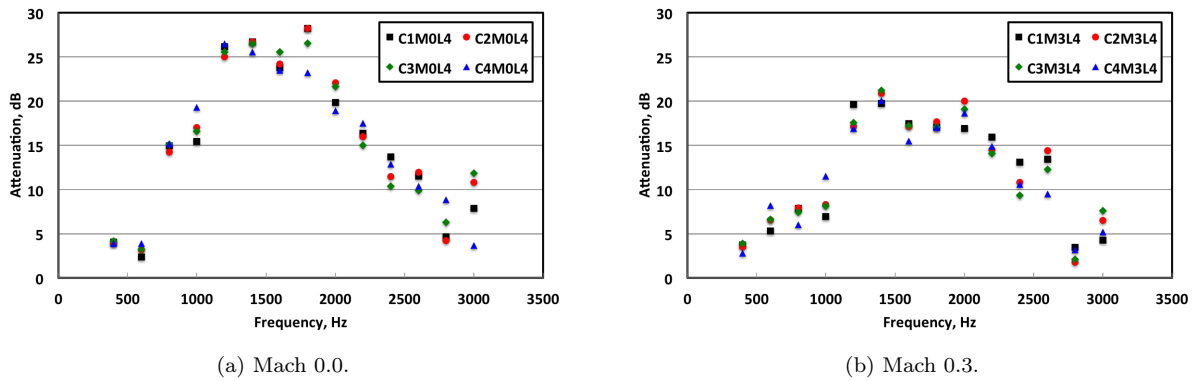


Figure 7: Attenuation spectra for C1 - C4 liners.

Figures 8 - 10 provide SPL axial profiles for the same four frequencies (1000, 1400, 1800, 2200 Hz) for the C2, C3, and C4 liners, respectively. These data were acquired with a source SPL of 140 dB, at flow Mach numbers of 0.0 and 0.3. The results for the C2 and C3 liners are nearly identical. As the only difference between these two liners is the use of bent chambers in the C3 liner to replace the longest chambers of the C2 liner, this further confirms that bent chambers can be used with confidence in future liner designs.

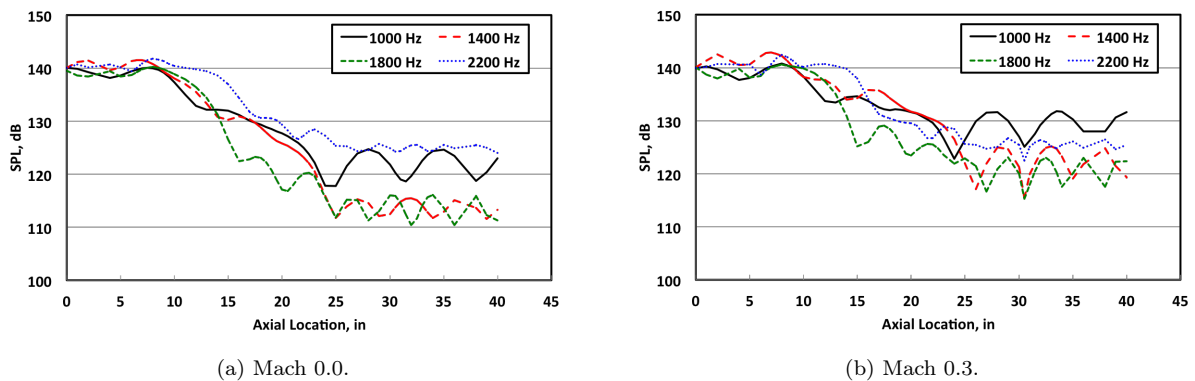


Figure 8: SPL axial profile for C2 liner. 140 dB source.

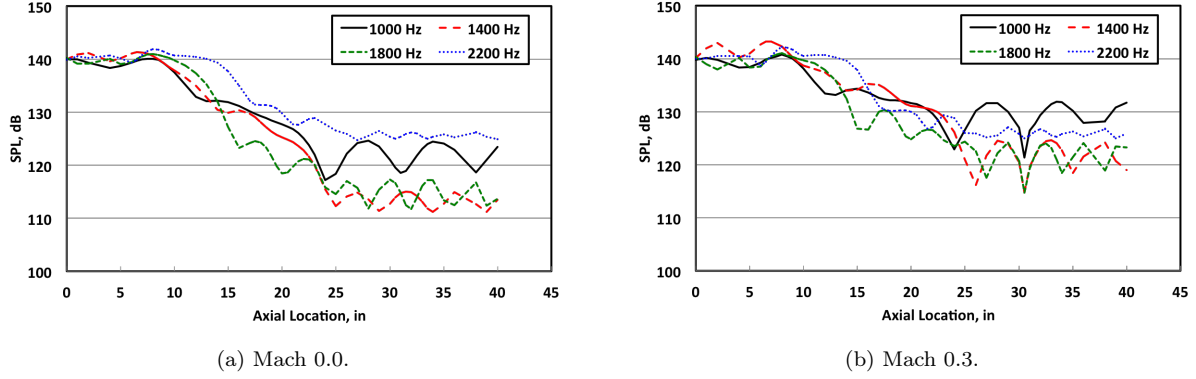


Figure 9: SPL axial profile for C3 liner. 140 dB source.

The results for the C4 liner are very similar, but the comparison with C2 liner results is slightly less favorable than is observed with the C3 liner results. This suggests that the effects of chamber ordering are not completely negligible, but are not large enough to cause any real concern, at least for the conditions considered in the GFIT tests of this study.

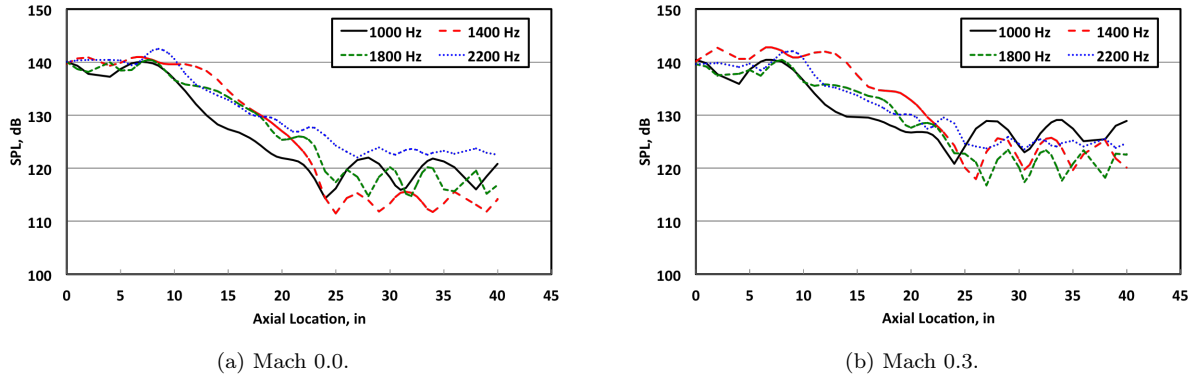


Figure 10: SPL axial profile for C4 liner. 140 dB source.

B. Curved Duct Test Rig Prediction Results

Six liner configurations shown in Figure 5 were evaluated with the CDL propagation code. Each liner configuration was evaluated with four different modal sources^c ($\{0,0\}$, $\{1,0\}$, $\{2,0\}$, and $\{0,1\}$), for the Mach 0.0 condition, and for source frequencies of 800, 1000, 1250, 1600, 2000, and 2500 Hz (1/3-octave band center frequencies to cover approximately two octaves).

Figure 11 provides SPL profiles for the Zone1 configuration, for each source type. These SPLs correspond to readings that would be expected for microphones located in the upper wall of the CDTR, 2.0" from the left wall (facing downstream). This is the spanwise location of the microphones that are currently in the lid array (see Fig. 4). As noted earlier, the CDL code does not capture reflections, as evidenced by the lack of standing wave patterns in the upstream ($x \leq 9.0$ ") and downstream ($x \geq 39.0$ ") hardwall sections of the CDTR. Even at the frequencies of maximum absorption, the attenuation predicted for this liner is much less than observed in the data measured with the liners optimized for the GFIT. There are two main causes of this reduction in sound absorption. First, the ratio of the liner length to duct width (compare to ratio of liner length to duct height for the GFIT) is 5 for the CDTR and 6.7 for the GFIT. More importantly, the cross-sectional area of the CDTR is eighteen (18) times larger than that of the GFIT. Each of these factors causes the amount of attenuation in the CDTR to be reduced relative to that of the GFIT.

^cThroughout this paper, modes are provided in the $\{m,n\}$ format, where m and n represent the vertical and horizontal mode orders, respectively.

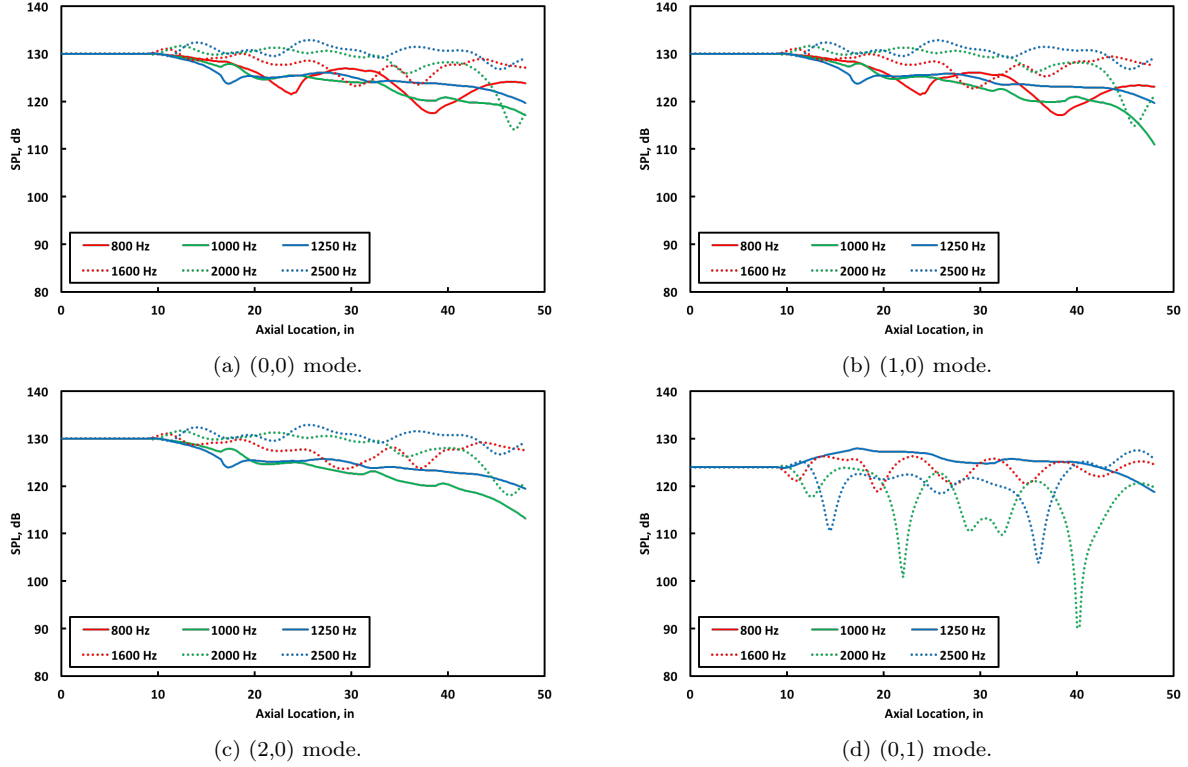
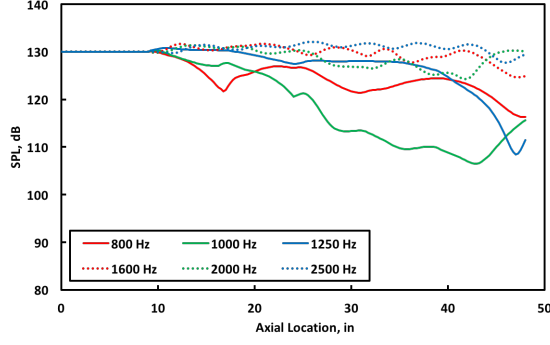


Figure 11: Effects of source mode on SPL axial profiles for liner configuration Zone1.

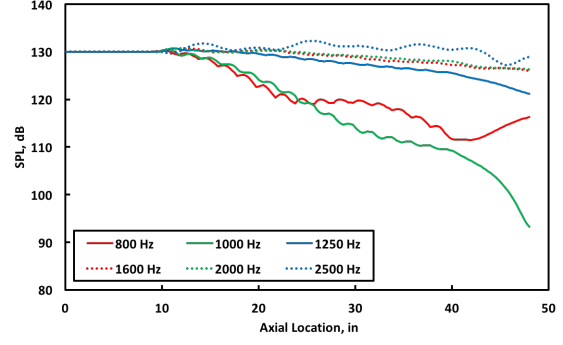
SPL profiles predicted for the first three source configurations ($\{0,0\}$, $\{1,0\}$, and $\{2,0\}$) are very similar across the full frequency range (the $\{2,0\}$ mode is cut off at 800 Hz). However, when the $\{0,1\}$ mode is employed (cut off at 800 and 1000 Hz), the predicted SPL profiles are noticeably different. The first three sources ($\{0,0\}$, $\{1,0\}$, and $\{2,0\}$ modes) are all zero-order in the spanwise dimension (i.e., between the liner and the hardwall on the opposite side of the duct), whereas the last source ($\{0,1\}$ mode) varies in the spanwise dimension.

Figure 12 provides SPL profiles for the ZoneR (reverse orientation of Zone1 configuration) and Distrib (redistribution of chambers from the Zone1 configuration) configurations, for the $\{0,0\}$ mode. A comparison of the results for the ZoneR and Zone1 configurations clearly indicate the orientation of the liner has an effect on the predicted SPL profiles, especially at the lower frequencies. These effects are significantly subdued at the higher frequencies. The Distrib configuration is shown to provide significantly different SPL profiles from those of the Zone1 configuration at the lower frequencies. Indeed, the Distrib configuration provides more attenuation than the Zone1 configuration for a number of test conditions, particularly at these lower frequencies. The differences are less significant at the higher frequencies.

The overall sound power level attenuation spectra are provided in Figure 13. The CDL code integrates the power across the source (9.0" upstream of the liner leading edge) and exit (9.0" downstream of the liner trailing edge) planes, and computes the attenuation as the difference between the two sound power levels. Although the SPL profiles differ between the various liner configurations, the attenuation spectra are relatively similar at the higher frequencies when a zero-order horizontal mode ($\{0,0\}$, $\{1,0\}$, or $\{2,0\}$) is employed (Fig. 13). This favorable comparison holds for all six liner configurations. At the lower frequencies, however, there is significant variability. Also, the attenuation spectra observed for the $\{0,1\}$ mode (Fig. 13d) are significantly different. Clearly, the orientation of the mode makes a difference.

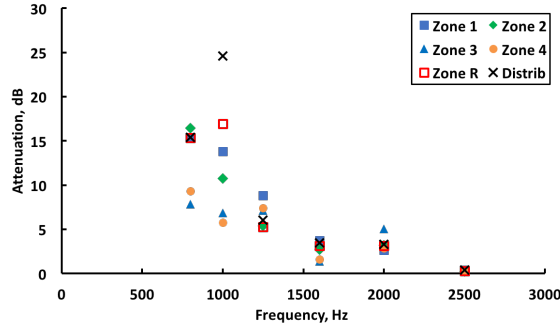


(a) Liner configuration ZoneR (reverse orientation).

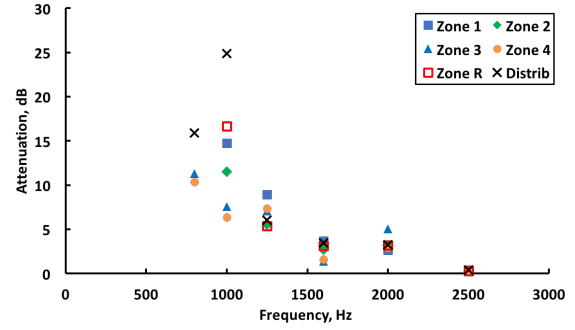


(b) Liner configuration Distrib (redistributed chambers).

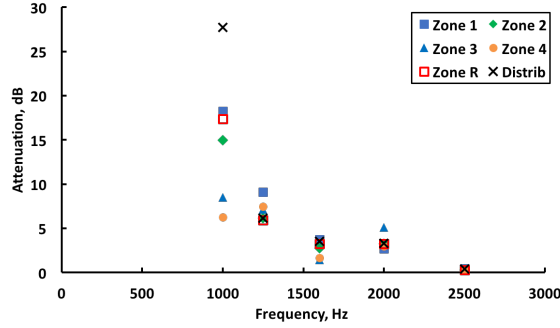
Figure 12: SPL axial profile for liner configurations ZoneR and ZoneD.



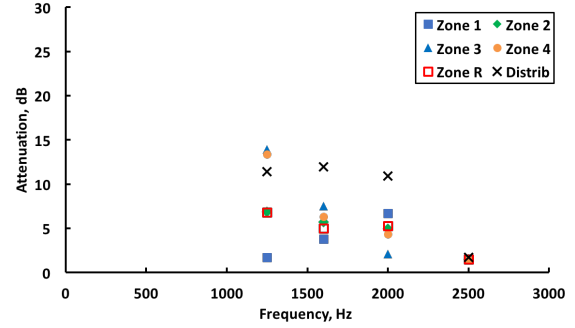
(a) Mode $\{0,0\}$.



(b) Mode $\{1,0\}$.



(c) Mode $\{2,0\}$.



(d) Mode $\{0,1\}$.

Figure 13: Effects of source modal content on attenuation spectra predicted for six CDTR liner configurations.

Overall, these results suggest that the distribution of the chambers for a variable-depth liner, whether by reordering the axial segments or by redistributing the individual chambers, should be included in the design process. However, as the frequency is increased, the effects of reordering are significantly reduced. The results for the Distrib configuration are also quite encouraging, as they suggest that reordering to enable use of bent chambers (and thus, to reduce total liner depth) is appropriate for more complex aeroacoustic environments such as are present in the CDTR.

V. Concluding Remarks

Four liner configurations were evaluated in the GFIT, for which only plane waves are present in the upstream and downstream rigid wall sections over the majority of the frequency range of interest (400 to 3000 Hz). The first configuration (C1) was an axially-segmented (zone) liner for which the chamber depths of

each axial segment were optimized to maximize attenuation from 1000 to 3000 Hz. The second configuration (C2) was designed to use the same chamber depths as the C1 liner, but with the chambers interleaved within each pair of axial segments. The third configuration employed bent chambers to reduce the total depth, but was otherwise identical to the C2 liner. Finally, the last configuration (C4) consisted of the same set of chambers, but with chambers reordered to achieve an overall minimum depth. The following conclusions can be drawn from the results achieved with the C1 - C4 liners.

- Ordering of chambers within an axially variable-depth liner has a definite effect on the axial SPL profiles measured at frequencies across the range of interest (400 to 3000 Hz).
- The overall attenuation (difference in SPL between the source and exit planes) is weakly dependent on chamber ordering.
- Bent chambers can be successfully used to reduce the overall liner depth with minimal effects on the attenuation.

It is important to note that these observations are based on data acquired in the GFIT, for which only plane waves exist in the upstream and downstream rigid wall sections over the majority of the frequency range of interest. A numerical study was conducted to explore the effects of higher-order modes.

The CDL code was combined with an optimizer developed using the Python programming language^{12,13} to design a zone liner for the CDTR with four axial segments. Four additional liners were designed based on simple reordering of the four segments. Also, one additional liner (total of six CDTR liners) was designed based on a redistribution of the individual chambers contained in the first design. Each of these liner configurations was evaluated numerically using the CDL propagation code. The following conclusions can be drawn from this numerical study.

- Results predicted for these six CDTR liners (Zone1 - Zone4, ZoneR, Distrib) are generally similar to those observed with the GFIT liners when the source consists of the $\{0,0\}$, $\{1,0\}$, or $\{2,0\}$ mode (i.e., zero-order mode between the liner and opposing hardwall). Specifically, the axial SPL profiles are predicted to vary with liner configuration, especially at the lower frequencies (800 and 1000 Hz). As with the GFIT results, the overall attenuation (difference in sound power level between the source and exit planes) is dependent on the axial distribution of chambers, but this effect is not generally significant. The attenuation spectra exhibit minimal variability for each of these three sources.
- For those cases where the $\{0,1\}$ mode is employed, the predicted results are noticeably different from those achieved with the other modal sources. This is observed both in the axial SPL profiles and in the overall attenuation spectra. When this source is employed, the effects of chamber reordering are greatly magnified. However, it is noted that each of the five four-segment liners (Zone1 - Zone4 and ZoneR) provides similar overall attenuation at the higher frequencies (i.e., for frequencies well away from cut on).
- Results predicted for the Distrib configuration (chambers redistributed to maximum extent) suggest that it is acceptable to configure the liner to take advantage of bent chambers, thereby reducing the overall depth of the liner.

A few items are proposed for further investigation. First, a few of the CDTR liner configurations should be built and tested in the CDTR. These tests should include a variety of sources (one or more modes), and should be conducted with and without grazing flow. Finally, recall that the CDL code is based on a parabolic approximation to the convected Helmholtz equation. Thus, it would be useful to compare the CDL predictions and CDTR measurements with predictions using the CHE propagation code, for which the reflections could be taken into account.

Finally, it is perhaps worth noting the obvious. Axially variable-depth liners offer the potential to provide improved fan noise reduction relative to the uniform-impedance liners typically used in current commercial aircraft. Based on the limited cases investigated thus far, this conclusion appears to hold regardless of whether the axially variable depths are achieved via a distributed array of chambers (where the depths vary from chamber to chamber) or a group of zones (groups of chambers for which the depth is constant). It also appears to hold regardless of complexity of the aeroacoustic environment in which the liner is placed. Clearly, axially variable-depth liners warrant further investigation.

Acknowledgments

The authors wish to express sincere appreciation to Martha Brown, Carol Harrison, and Larry Becker for their efforts in the acquisition of the GFIT data, and to Rob Andrews of the Additive Manufacturing Center for his efforts in the fabrication of the GFIT liners. The Advanced Air Transportation Technologies Project of the NASA Advanced Air Vehicle Program funded this work.

References

- ¹Kraft, R. E., "Theory and Measurement of Acoustic Wave Propagation in Multi-Sectioned Rectangular Ducts," Ph.D. Dissertation, University of Cincinnati, Cincinnati, OH, May 1976.
- ²Sawdy, D. T., Beckemeyer, R. J., and Patterson, J. D., "Analytical and Experimental Studies of an Optimum Multisegment Phased Liner Noise Suppression Concept," NASA CR 134960, 1976.
- ³Howe, M. S., "The attenuation of sound in a randomly lined duct," *Journal of Sound and Vibration*, Vol. 87, No. 1, 2006, pp. 83–103.
- ⁴Watson, W. R., "An Acoustic Evaluation of Circumferentially Segmented Duct Liners," *AIAA Journal*, Vol. 22, No. 9, 1984, pp. 1229–1233.
- ⁵Lan, J. H., "Turbofan Duct Propagation Model," NASA CR 211245, 2001.
- ⁶McAlpine, A., Astley, R. J., Hii, V. J. T., Baker, N. J., and Kempton, A. J., "Acoustic scattering by an axially-segmented turbofan inlet duct liner at supersonic fan speeds," *Journal of Sound and Vibration*, Vol. 294, No. 4-5, 2006, pp. 780–806.
- ⁷Jones, M. G., Watson, W. R., Nark, D. M., and Howerton, B. M., "Evaluation of a Variable-Impedance Ceramic Matrix Composite Acoustic Liner," AIAA Paper 2014-3352, June 2014.
- ⁸Jones, M. G., Watson, W. R., Nark, D. M., and Howerton, B. M., "Evaluation of Variable-Depth Liner Configurations for Increased Broadband Noise Reduction," AIAA Paper 2015-2697, June 2015.
- ⁹Jones, M. G., Watson, W. R., Nark, D. M., Schiller, N. H., and Born, J. C., "Optimization of Variable-Depth Liner Configurations for Increased Broadband Noise Reduction," AIAA Paper 2016-2783, May 2016.
- ¹⁰Watson, W. R., Jones, M. G., and Parrott, T. L., "Validation of an Impedance Eduction Method in Flow," *AIAA Journal*, Vol. 37, No. 7, July 1999, pp. 818–824.
- ¹¹Nark, D. M. and Jones, M. G., "Broadband Liner Optimization for the Source Diagnostic Test Fan," AIAA Paper 2012-2195, June 2012.
- ¹²"URL: <http://www.python.org>," [cited 25 March 2016].
- ¹³Jones, E., Oliphant, T., Peterson, P., et al., "SciPy: Open source scientific tools for Python," URL: <http://www.scipy.org/>, 2001–.